Zootaxa 4227 (2): 219–232
http://www.mapress.com/j/zt/

Article

ISSN 1175-5326 (print edition)
ZOOTAXA
ISSN 1175-5334 (online edition)

https://doi.org/10.11646/zootaxa.4227.2.4
http://zoobank.org/urn:lsid:zoobank.org:pub:2F7098A1-FE97-48BD-A8B3-321D4569FFAE

Osteology of *Physalaemus nattereri* (Anura: Leptodactylidae) with comments on intraspecific variation

JÉSSICA FRATANI[1,2], MANOELA WOITOVICZ-CARDOSO[2]
& ANA CAROLINA CALIJORNE LOURENÇO[3]

[1]*Unidad Ejecutora Lillo-CONICET, Miguel Lillo, 251-4000, San Miguel de Tucumán, Argentina. E-mail: jessicafratani@gmail.com*
[2]*Setor de Herpetologia, Departamento de Vertebrados, Museu Nacional, Universidade Federal do Rio de Janeiro. Quinta da Boa Vista 20940-040. Rio de Janeiro, RJ, Brasil. E-mail: manoelawcardoso@gmail.com*
[3]*Instituto de Biociências, Departamento de Zoologia, Jacarezário. Universidade Estadual Paulista Júlio de Mesquita Filho - UNESP . 13506-900 - Rio Claro, SP, Brasil. E-mail: carolcalijorne@gmail.com*

Abstract

The cranium, postcranium, and osteological variation of *Physalaemus nattereri* (Steindachner) are described. The main sources of variation involve the degree of mineralization of the nasal capsule and the lengths of dermal skull bones (e.g., vomer, sphenethmoid, and neopalatine). Osteologically, *P. nattereri* differs from its congeners by the anterior placement of the jaw articulation (which lies anterior to the intersection between the alae and cultriform process of parasphenoid), and by the separation of the frontoparietals from the anterior margins of exoccipitals. Descriptions of the nasal capsule, the auditory apparatus, and the iliosacral articulation are presented for the first time for this species. One putative morphological synapomorphy is presented for the *P. signifer* Clade.

Key words: Amphibia, morphology, anatomy, skeleton, nasal capsule

Introduction

Physalaemus nattereri is a conspicuous species, known especially for its deimatic behavior—i.e., body-raised with legs vertically stretched and possession of eyespot-like glands (Sazima & Caramaschi 1986; Toledo *et al.* 2011). It is a fossorial and seasonal species that is distributed in open areas of Brazil, eastern Paraguay, and eastern Bolivia (Aquino *et al.* 2004).

Physalaemus nattereri was first described as *Eupemphix nattereri* Steindachner; at the time, the absence of maxillary and premaxillary teeth in *Eupemphix* was used to differentiate it from *Physalaemus* Fitzinger (Boulenger 1888). Lynch (1970) combined *Engystomops* Jiménez de la Espada, *Eupemphix* Steindachner, and *Physalaemus* Fitzinger into a single genus, and grouped *P. nattereri* with *P. albifrons* (Spix), *P. biligonigerus* (Cope), *P. fuscomaculatus* (Cope), and *P. santafecinus* (Barrio) based on its body size, marbled dorsal pattern, and other external morphological traits. In a phenetic taxonomic revision of *Physalaemus*, Nascimento *et al.* (2005) rearranged the genus into seven species groups (*P. cuvieri* Fitzinger, *P. signifer* (Girard), *P. albifrons*, *P. deimaticus* Sazima & Caramaschi, *P. gracilis* (Boulenger), *P. henselii* (Peters), and *P. olfersii* (Lichtenstein & Martens)), placed the *P. pustulosus* (Boulenger) species group (sensu Lynch 1970) in *Engystomops* and *P. nattereri* in *Eupemphix*. *Eupemphix* was distinguished from *Physalaemus* and *Engystomops* by its possession of the following combination of osteological features: skull-mandible articulation anterior to the intersection between the alae and cultriform process of parasphenoid (first observed by Lobo 1996); frontoparietals not overlapping the anterior margins of exoccipitals; and presence of quadratojugals (Nascimento *et al.* 2005).

The phylogenetic hypotheses that include *Physalaemus nattereri* are based on molecular evidence (from mitochondrial and nuclear gene sequences), and in most of these studies, *Physalaemus nattereri* is inferred to be the sister taxon of *P. signifer* species group (Pyron & Wiens 2011; Faivovich *et al.* 2012; Fouquet *et al.* 2013; de Sá

Accepted by D. Baldo: 29 Nov. 2016; published: 2 Feb. 2017

et al. 2014; Pyron 2014). Lourenço *et al.* (2015) published a phylogeny of *Physalaemus* and proposed a new combination for *Physalaemus signifer* Clade that comprises *P. nattereri* and the species in the *Physalaemus signifer* and *P. deimaticus* groups, *sensu* Nascimento *et al.* (2005).

Osteological characters play a large role in the differentiation of the currently recognized anuran taxa (Trueb 1973), and have been included in several taxonomic studies of species within *Physalaemus* (e.g., Lobo 1992, 1995, 1996; Lynch 1970; Lynch 1971; Nascimento *et al.* 2005). However, the osteology of only few taxa have been thoroughly described, and no one has addressed the intraspecific variation of adults. Consequently, there are few baseline studies to provide reliable information for taxonomic, phylogenetic, and morphological assessments of this diverse anuran group. Herein, we provide a detailed osteological description of *Physalaemus nattereri* and explore two topics more closely—viz., intraspecific variation in, and significance of, osteological features.

Material and methods

One female and sixteen males from nine different populations (Appendix I) were examined. All specimens are deposited in the Amphibian Collection of the Museu Nacional, Universidade Federal do Rio de Janeiro (MNRJ). Based on the presence of mature gonads and secondary sex characters externally visible (e.g., vocal sac in males), all individuals are adults. We endeavored to examine individuals in the same stage of development by selecting specimens with similar snout–vent lengths, although we realize that age and size are not directly related in all anurans (Halliday & Verrell 1988).

The authorities for the terminology used herein are, as follow: general osteological terminology fide Trueb (1973, 1993); olfactory capsule fide Pugener & Maglia (2007); and phalangeal, carpal and tarsal osteology fide Fabrezi (1992, 1993, 1996). The terms ossification and mineralization (= calcification) used in this study follow those of Trueb (1973). Ossification refers to the formation of endochondral and intramembranous bone, whereas calcification refers to the (secondary) deposition of minerals in a cartilaginous structure (Trueb 1973).

The clearing-and-staining protocol was adapted from Taylor & Van Dyke (1985). Snout–vent length was measured to the nearest millimeter (mm) with calipers with 0.05 mm precision. Drawings of the cranium were made using a Zeiss stereomicroscope with an attached camera lucida. Illustrations were based on images taken with an Olympus SZX7 stereomicroscope attached to an Olympus DP25 digital camera and with two fully automated stereo microscope Leica, M205 FA and M205 C, attached to Leica DFC450 digital camera.

Results

Osteology. The description below is based on examination of one adult male (MNRJ 13070), and it is followed by a consideration of intraspecific variation.

Cranium.—The skull bones are not ornamented (Fig 1A, 1B). The skull is wider than long, and its greatest width is at the level of the suspensorium. The width of the braincase increases gradually toward the posterior margin; at the midorbital level, the width of the braincase is approximately equal to its height.

The rostrum is one-third the total length of the skull (Fig 1C, 1D). The paired olfactory capsules are cone-shaped in dorsal view. The capsules are separated by a slender, partially ossified sagittal plate, the septum nasi. The roof of the nasal region is composed of a slender, cartilaginous tectum nasi, which is contiguous with the septum nasi medially. The anterior end of the tectum nasi has a round process, the median prenasal process. The floor is formed by a plate of cartilage, the solum nasi, which is a broadly connected to the septum nasi and mineralized medially. The postnasal wall is transverse to the longitudinal axis of the skull and separates the olfactory capsule from the orbit. It is contiguous with the sphenethmoid medially and has a well-developed process extending anteriorly at its midpoint; the height of the wall decreases in a medial to lateral direction. The lateral face of the postnasal wall, the planum triangulare, has two maxillary processes; the anterior process is not well-developed and the posterior process joins the anterior process of the pterygoid cartilage.

The anterior region of the nasal capsule lies at the level of the alary process of the premaxilla (Fig 1D). The semi-circular, oblique cartilage is dorsolateral to the septum nasi; it forms the posterior border of the fenestra endonarina and has a broad connection with the tectum nasi. Posterolateral and contiguous to the oblique cartilage,

the planum terminale extends ventrally and connects to the lamina inferior and the crista subnasalis. The planum terminale has a posterior and rod-shaped process, the lingular process. The superior prenasal cartilage is fused to the alary cartilage and extends anteriorly, investing the posterior region of the alary process of the premaxilla. The inferior prenasal cartilage projects from the solum nasi and underlies the alary process of the premaxilla through its length. The crista subnasalis is a V-shaped structure; the closed end is lateral. The dorsal surface is contiguous with the lamina inferior and planum terminale, whereas the ventral surface is contiguous with the solum nasi. The lateral tip of the crista subnasalis is bifurcate; the anterior branch extends to the premaxilla and the posterior branch to the maxilla. A rod of cartilage connects the crista subnasalis to the lingular process. The alary cartilage is a cup-shaped structure that lies anterior to the oblique cartilage and forms the anterior border of the nostril.

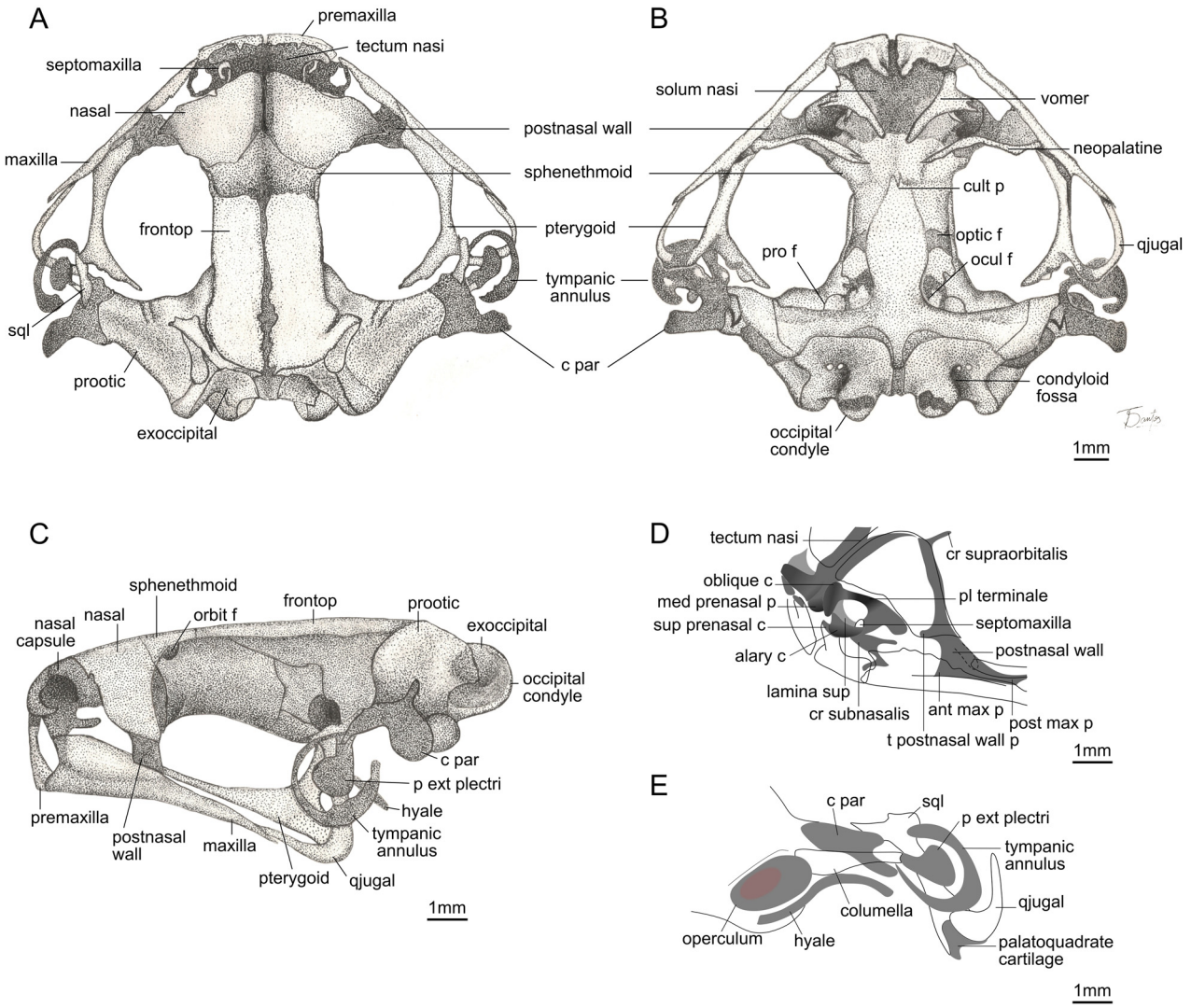

FIGURE 1. Skull of *Physalaemus nattereri* (MNRJ 13070) in (A) dorsal, (B) ventral, and (C) lateral views. Details of (D) the nasal capsule and (E) operculum. alary c, alary cartilage; ant max p, anterior maxillary process; c par, crista parotica, cr subnasalis, crista subnasalis; cr supraorbitalis, crista supraorbitalis; cult p, cultriform process of parasphenoid; frontop, frontoparietal; lamina sup, lamina superior; med prenasal p, median prenasal process; oblique c, oblique cartilage; ocul f, oculomotor foramen; optic f, optic foramen; orbit f, orbitonasal foramen; p ext plectri, pars externa plectri; pl terminale, planum terminale; post max p, posterior maxillary process; pro f, prootic foramen; qjugal, quadratojugal; sql, squamosal; sup prenasal c, superior prenasal cartilage; t postnasal wall p, triangular postnasal wall process.

The dermal septomaxilla lies within the olfactory capsule (Trueb 1993). The bone can be observed at the edge of the external naris, posterior and ventral to the alary cartilage. In dorsal view, the septomaxilla is U-shaped and the closed end is oriented ventrolaterally. The septomaxilla has three projections. The anterior ramus is slender, acuminate, and slightly shorter than the posterior ramus. The posterior ramus is broad with a rounded terminus. The anterior region of the septomaxilla has a ventral projection that extends posteriorly, and has the same length as the

anterior ramus. On the right side of the specimen examined, the ends of the posterior ramus and the ventral projection of the septomaxilla are connected posterolaterally.

Braincase.—Posterior to the olfactory capsules, the sphenethmoid forms the dorsal, ventral, and lateral braincase walls. Ventrally it is partially overlapped by the cultriform process of the parasphenoid, the neopalatines, and the vomers. Dorsally, the sphenethmoid is overlapped by the posterior borders of the nasals, and the anterior borders of the frontoparietals. The posterior edge of the bony sphenethmoid lies approximately at the level of the midorbit. The orbitonasal foramen is dorsolateral and completely enclosed by the sphenethmoid. The optic, oculomotor, and prootic foramina are positioned ventrally at the posterior region of the braincase. The optic fenestra is broad, bordered by the lateral of the cultriform process of the parasphenoid, cartilage, and the prootic. The oculomotor foramen is completely enclosed in cartilage. The prootic foramen is bordered by the prootic laterally and by cartilage medially.

The prootics and exoccipitals are indistinctly fused at the posterior region of the braincase. The prootic is triangular and lateral; it forms the otic capsule. Its dorsomedial margin is overlapped by the posterior end of the frontoparietal. Dorsally, the epiotic eminence and the otic crest are well developed. Lateral to the prootic region, the crista parotica is cartilaginous, well developed, and has a teardrop-shaped expansion.

The occipital artery (carotid artery of Lynch, 1971) courses rostrad through the occipital canal dorsally. The canal is partially roofed by the posterior end of the frontoparietal over the otic region; it is oriented slightly diagonal to the longitudinal axis of the skull.

The exoccipitals form the posteromedial region of the otic capsule, between the prootics. The exoccipital articulates with the vertebral column via a pair of bean-shaped, ventrolateral condyles, which are widely separated. The occipital condyles are well developed, convex, and the articular surface is partially cartilaginous. Lateral to each condyle there is a wide condyloid fossa, which bears a large jugular foramen positioned on the medial wall. The superior perilymphatic foramen is located on the posterior wall of the otic capsule anterior to the jugular foramen and medial to the inferior perilymphatic foramen.

Dermatocranium.—The paired nasals roof the nasal capsules. They have a trapezoidal shape and a convex dorsal surface. The maxillary process is well developed, but not in contact with the pars facialis of the maxilla; it forms a bony margin for the medial three quarters of the orbit. Posteromedially, the nasals overlap the anterior margin of the sphenethmoid, but are not in contact with the frontoparietals.

The paired frontoparietals roof the brain case, are well developed, and have approximately the lenght of the skull. The bones are narrowly separated medially; thus, the frontoparietal fontanelle is not exposed. The posterior region of the frontoparietals invests the braincase and terminates posteriorly at the level of the exoccipitals.

The parasphenoid is an inverted T-shaped bone that underlies the braincase. The cultriform process of the parasphenoid overlaps the sphenethmoid anteriorly, and extends to the level of the orbitonasal foramina. Its lateral margins are convex; they are widest at the level of the optic foramen, and gradually converge anteriorly. The parasphenoid alae are about the same length as the cultriform process, and are not fused with sub-adjacent bones. Each ala is laterally oriented and underlies the otic capsule. The posteromedial process is well developed, triangular, and does not extend to the foramen magnum.

The long, slender neopalatines are transversely oriented to the longitudinal axis of the skull and slightly bowed. Ventrally, the neopalatines overlap the postnasal wall, the sphenethmoid medially, and the anterior process of the pterygoid laterally.

The paired vomers underlie the floor of the olfactory capsule. Each vomer bears an anterior, prechoanal, postchoanal, and posterior process. The broad anterior process extends anterolaterally, but has no contact with the premaxilla and the maxilla. The well-developed prechoanal process is about the same size as the anterior process and is acute and triangular. The slender postchoanal process extends over about half of the medial border of the choana. The posterior process is slender, transversally oriented and overlaps the sphenethmoid.

Upper Jaw.—The upper jaw is complete and comprises the premaxillae, maxillae, and quadratojugals. None of these components is fused to an adjacent element or bears teeth. The paired premaxillae are narrowly separated from one another at the midline. The dorsolateral face of the pars palatina of the premaxilla slightly overlaps the pars palatina of the adjacent maxilla. The alary process of premaxilla is rectangular and perpendicular to the longitudinal axis of the skull. The medial margins of the alary processes parallel one another. The palatine process of the pars palatina is well developed, extends posterodorsally, and is acuminate.

The maxillae are the largest structures of the maxillary arcade, representing more than half of the total length

of the skull. The anterior end of the maxilla overlaps the labial surface of the premaxilla; posteriorly, it articulates with the quadradojugal. The pars palatina of the maxilla is a horizontal palatal shelf that extends along the anterior two thirds the length of the maxilla. The anterior end of the pars palatina is invested ventrally by the crista subnasalis, and posteriorly by the neopalatines and the anterior process of the pterygoid. The pars facialis is the dorsal component of the maxilla that extends from the anterior region of the maxilla to the level of the planum triangulare; its height is equivalent to that of the alary process of the premaxilla.

The slender quadratojugal is slightly concave, rod-shaped, and has approximately one third of the total length of the maxilla. It completes the maxillary arcade posteriorly, investing the ventrolateral surface of the pars articularis of the palatoquadrate and the ventral ramus of the squamosal.

Suspensory apparatus.—The paired, T-shaped pterygoids brace the maxillary arcade. All processes of the pterygoid are well developed; the medial and posterior processes are approximately half the length of the anterior process. The anterior process extends over the pars palatina to meet the maxilla at about its mid-length; the process overlaps the pterygoid process of the palatoquadrate cartilage. The medial process invests the pseudobasal process of the palatoquadrate cartilage and has no bony contact with the otic capsule. The posterior process joins the quadratojugal-squamosal complex.

The paired squamosals are T-shaped in lateral aspect. The anterior zygomatic ramus extends toward the maxilla and is about half the length of the otic ramus. The otic ramus is posteriorly acuminate and overlaps the lateral margin of the crista parotica; an otic plate is absent. The ventral ramus invests the palatoquadrate cartilage and articulates with the quadratojugal. It is straight and oriented at a 45˚ angle to the jaw.

The palatoquadrate remains cartilaginous in adults and is invested by the pterygoid, quadratojugal, and squamosal bones. The ventral surface of the palatoquadrate cartilage forms the pars articularis—the articulation point of the upper and lower jaws. The pars articularis is completely cartilaginous. The otic process extends dorsally, through the internal surface of the descendent ramus of the squamosal, and connects to the crista parotica. A slender cartilaginous process connects the otic process and the pars externa plectri.

Auditory Apparatus.—The tympanum is supported internally by the tympanic annulus, which is a concave, funnel-shaped cartilage that overlaps the ventral ramus of the squamosal (Fig 1E). The tympanic annulus is incomplete dorsally, and neither of its ends joins the crista parotica. The teardrop-shaped pars externa plectri is positioned centrally within the tympanic annulus, and is half the length of the columella. The long, slightly bowed columella is an ossified stylus formed by the synostotic fusion between the pars media plectri and the pars interna plectri. The footplate of the columella is expanded and meets the fenestra ovalis anterodorsally to the operculum. The operculum is an externally convex, oval, cartilaginous structure that covers almost completely the oval window. A well-developed opercular crest extends medially through the wider diameter of operculum.

Lower Jaw.—The mentomeckelians are paired, cylindrical bones in the anteromedial region of the lower jaw (Fig 2A). The medial ends of the mentomeckelians remain cartilaginous in the adult, and are connected medially by ligaments forming the mandibular symphysis. A slender dentary, which lacks odontoids or serrations, forms the anterolateral margin of the mandible and laterally invests Meckel's cartilage over the anterior half of the mandible. The angulosplenial invests the lingual and ventral face of Meckel's cartilage; it is the major bone of the mandible, extending from the proximity of lateral end of the mentomekelians to the pars articularis. Posteriorly, the pars articularis remains cartilaginous, and the mandible is slightly curved medially at the prearticular region. The coronoid process is small, arcuate, and positioned in the posterior region of the anlgulosplenial.

Hyolaryngeal apparatus.—The hyoid is cartilaginous, and the width at narrowest point of the hyoid corpus is approximately equal to its total length (Fig 2A). The hyoglossal sinus is U-shaped and it deepens up to a third the length of the anterolateral processes. The slender, curved hyali connect the hyoid to the skull. Each hyale extends anteriorly from the anterolateral margin of the hyoid plate, curves posterodorsally, and extends to the anteroventral region of the otic capsule. The anterior processes are short, and originate from the anterior curvature of the hyali. The anterolateral processes are broad lobes with a wide connection to the hyoid corpus. The slender, laterally oriented posterolateral processes originate from the posterolateral margins of the hyoid. The posterior margins of the posterolateral processes extend slightly over the posterior border of the hyoid. The posteromedial processes are slender, rod-shaped bones that lie medial to the posterolateral processes. Each posteromedial processes diverges 45˚ laterally from the longitudinal axis of the body. The anterior and posterior ends of the posteromedial processes are slightly expanded. The posteromedial processes are ossified but the distal epiphysis remains cartilaginous, and the region between the anterior epiphyses is greatly mineralized.

The laryngeal cartilages are represented by a globular structure, positioned between the posteromedial processes of the hyoid (Fig 2A, 2B). The valve-shaped arytenoids protrude posteriorly toward the cardiac end. The cricoid cartilage is a circular ring, which is completely ventral. The articular process of the cricoid ring is in contact with the arytenoid cartilages. The esophageal process is very short and lacks a muscular process. The cardiac process is a wide plate; it has an anterior projection that folds out and extends to a prominent structure on its medial surface. Each arytenoid cartilage bears a small ventral projection that is oriented toward the cricoid ring. The bronchial processes are parallel, rod-shaped structures, with bifurcate termini.

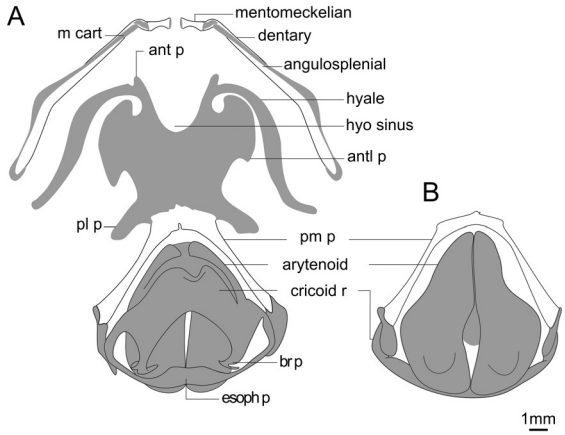

FIGURE 2. Mandible, hyoid, and laryngeal cartilages of *Physalaemus nattereri* (MNRJ 13070). (A) Ventral view. (B) Dorsal view. ant p, anterior process of the hyale; antl p, anterolateral process of the hyale; br p, bronchial process; cricoid r, cricoid ring; esoph p, esophageal process; hyo sinus, hyoglossal sinus; m cart, meckel's cartilage; pl p, posterolateral process; pm p, posteromedial process.

Axial skeleton.—The vertebral column is composed of eight procoelus presacral vertebrae, the sacrum, and the urostyle (Fig 3A). The atlas is not fused to the adjacent vertebrae. The cervical cotyles are oval and are oblique position oriented with respect to the main axis of the body and correspond to Type-I cotylar arrangement described by Lynch (1971).

The surfaces of the articular ends of the centra are concave anteriorly and convex posteriorly, as is characteristic of procoelus centra. The vertebrae decrease markedly in size towards the posterior end. The relative lengths of the transverse processes, in descending order, are III ≈ IV > V ≈ VI ≈ VII > VIII ≈ II. The transverse processes of the Presacrals III and VI are approximately perpendicular to the longitudinal body axis. Those of the Presacrals II, VII, and VIII are anterolaterally oriented. And the transverses processes of the Presacrals IV and V are posterolaterally oriented.

The sacral diapophyses are approximately the same length as Presacrals III and IV, and are posterolaterally oriented. The width of each sacral diapophysis increases slightly toward the lateral ends.

The long, slender urostyle is slightly shorter than the total length of the presacrals. It is well ossified, but the posterior end remains cartilaginous. The urostyle bears a dorsal longitudinal crest that extends through most of its length, and has a bicondylar articulation with the sacrum. The ridge is higher anteriorly and decreases in height gradually towards the posterior end. The rudiments of the neural canal were not observed.

Appendicular skeleton. *Pectoral girdle*.—The girdle is arciferal (Fig 3B). The pectoral fenestra is teardrop-shaped, with its length being approximately equal to its width, and the longitudinal axis of the fenestra lying transverse to the vertebral column. It is bordered anteriorly by procoracoid and clavicle, and posteriorly by the epicoracoid.

The omosternum is cartilaginous and slightly expanded anteriorly with a semicircular shape. The rod-shaped episternum is mainly cartilaginous with a light mineralization in its posterior region. The procoracoids are paired cartilaginous structures that are adjacent to the clavicles, and form the anterior margin of the pectoral fenestra. The procoracoids are contiguous to the epicoracoids medially, and laterally they extend up to half of the clavicles total

length. The epicoracoids are two C-shaped cartilages that lie at the central region of the pectoral girdle, and connect the clavicle and coracoids. In the specimen examined, the right epicoracoid overlaps the left, and the internal margins of the epicoracoids are heavily mineralized. Epicoracoidal horns are absent. The mesosternum is mostly ossified, except its anterior end, which remains cartilaginous. The margins of this element gradually narrow posteriorly up to about three quarters of its total length where the mesosternum bifurcates. There are two semicircular-shaped xiphisterna, each of which is connected to one of the mesosternum tips. Furthermore, both have mineralized deposits on their anterior regions and have inner prolongations in the lateral borders.

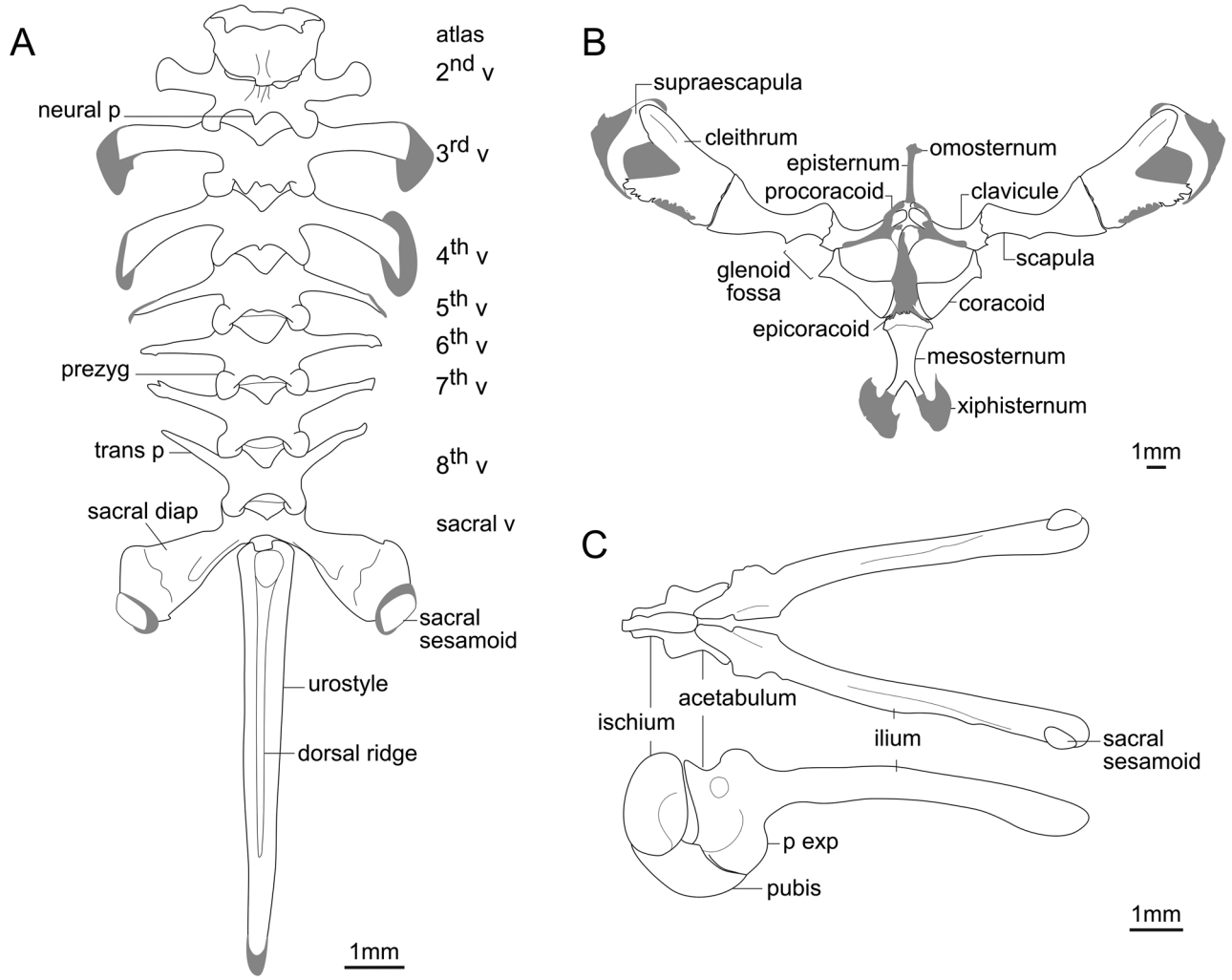

FIGURE 3. Axial and appendicular structures of *Physalaemus nattereri* (MNRJ 13070). (A) Vertebral column in dorsal view. (B) Shoulder girdle in ventral view and (C) pelvic girdle in dorsal and lateral views. neural p, neural process; p exp, preacetabular expansion; prezyg, prezygapophysis; sacral diap, sacral diapophysis; trans p, transverse process; v, vertebra.

The clavicles are bow-shaped with the anterior sides being concave. The medial tip of each clavicle is slightly separated from its counterpart and the glenoid end is slightly expanded and joins the pars acromialis of the scapula. The coracoid, which is approximately the same size as the scapula, is rectangular and its ends are expanded so that they are twice the width of the mid-shaft of the bone. The glenoid end of the coracoid is wedge shaped. The scapula is approximately half the clavicle length, and twice its width. It is rectangular and its ends are expanded. The anterior margin of the glenoid end of the scapula has a convex expansion, the pars acromialis, and its posterior face bears the pars glenoidalis, which is concave and forms the glenoid fossa. The glenoid fossa is bordered by the scapula, coracoids, and clavicles.

The cleithrum is an ossified element contiguous with the suprascapula, which is cartilaginous but greatly mineralized. The lateral side of cleithrum is bifid, with the posterior ramus half the width and two thirds the length of the anterior ramus. The anterior ramus has a longitudinal ridge.

Pelvic girdle.—The ilial-sacral joint is Type IIA (sensu Emerson 1982) and elliptic sacral sesamoids are present on the distal margin of the diapophysis (Fig 3C). Together, the internal margins of the ilia configure a V-shape. Each ilium has a well-developed dorsal crest on the posterior two thirds of its length. It increases in height posteriorly and expands laterally near the acetabulum. Ventrally, the ilia have poorly developed preacetabular expansions. The ilia are fused with the ischium and the pubis, and together they form a spherical structure from a lateral view. The posterodorsal half of the acetabulum is composed by the ischium, which has a dorsal ridge that is greater in height to the ilial ridge. The pubis is cartilaginous but lightly mineralized. It forms the ventral portion of the acetabular region, between the ilium and the ischium. The acetabular portions of the ilium, ischium and pubis are approximately equal in size.

Forelimb.—The humerus bears a well-developed anterior crest that extends from the glenoidal head to a point approximately at the midlength of the bone (Fig 4A). Two other crests extend from the distal epiphysis over approximately the distal third of the humerus, one dorsal and one ventral. The distal and glenoidal heads of the humerus are about equal in size, rounded, and compressed. The radioulna is flattened; the sulcus intermedius is a distinct longitudinal groove, which starts at the distal head of the radioulna and extends to its midlength.

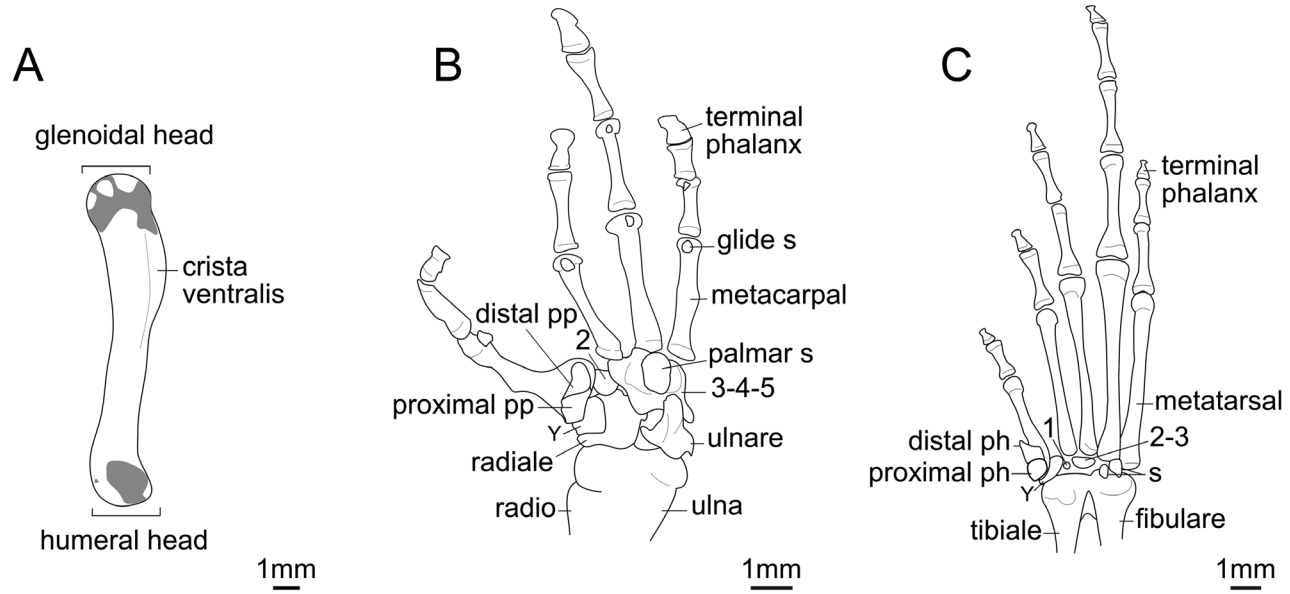

FIGURE 4. Limb structure of *Physalaemus nattereri* (MNRJ 13070). (A) Left humerus in dorsal view. (B) Left hand in ventral view and (C) left pes in ventral view. 1, tarsal 1; 2, carpal 2; 2–3, tarsal 2–3; 3–4–5, carpal 3–4–5; distal ph, distal element of prehallux; distal pp, distal element of prepollex; proximal ph, proximal element of prehallux; proximal pp, proximal element of prepolex; s, sesamoid; Y, Element Y.

The hand has five carpals and two prepollical elements representing Type C morphology of Fabrezi (1992) (Fig 4B). The phalangeal formula is 2–2–3–3, and the relative length of the fingers is IV > V > III ≈ II. A large, ossified palmar sesamoid is present on the ventral surface of the hand. Two small, ossified glide sesamoids lie on the distal head of each metacarpal, and on the distal head of the proximal phalanx of digits IV and V. The dorsal surface of the hand bears one spherical pararadial sesamoid over the distal head of the ulnare. The terminal phalanges are simple, with knobbed termini, and the metacarpal of the second digit bears a knoblike protuberance. The prepollex is well developed and composed of two segments, with no apparent additional cartilaginous elements. The proximal prepollical element is square and ossified, whereas the distal prepollical element is elongated and partially cartilaginous, and has a rounded terminus.

Hind limb.—The femur is about equal in length to the tibiofibula, whereas the tibiofibula is twice the size of the tibiale-fibulare. The tibiale and fibulare are distally and medially fused, although separated from each other in their proximal halves. One ossified graciella sesamoid, embedded in the tendon of the m. gracilis major, lies ventral to the distal head of the femur. One poorly developed and ossified cartilago sesamoides is embedded in the tendon of the m. plantaris profundus, and lies ventral to the proximal head of the tibiale-fibulare.

Three tarsal elements are present: Element Y, Distal Tarsal 1, and Distal Tarsal 2-3 (Fig 4C). Element Y joins the proximal and spherical element of the prehallux, which in turn is connected with the distal and drop-shaped element of the prehallux. Distal Tarsal 1 articulates with the Metatarsals I and II, and the Distal Tarsal 2–3 articulates with Metatarsals II and III. Metatarsals IV and V articulate directly with the fibulare. Two ossified, round plantar sesamoids lie on the ventral surface of the distal end of the fibulare. And one poorly developed glide sesamoid lies on the ventral surface of the distal ends of the Metatarsals I and II.

The relative lengths of the digits are IV > III > V > II > I. The digital phalangeal formula is 2–2–3–4–3. The terminal phalanges are knobbed. The prehallux has two segments with extensive mineralization; the distal segment is pointed.

Intraspecific variation. There are no remarkable differences in the shapes of skeletal structures among the specimens of *Physalaemus nattereri* examined at the intra- and interpopulational levels or between female and males. The osteological variation among males primarily involves the degree of mineralization and ossification of cartilaginous elements, and the sizes of some dermal bones (e.g., nasals, frontoparietals, neopalatines, and vomer). The variation of some structures is summarized in Table 1. Mineral deposition is not clearly related to the size of the individuals, because similar-sized frogs (40.7 mm ± 3.6 mm) have different degrees of mineralization.

TABLE 1. Intraspecific variation of osteological characters as observed in 16 male *Physalaemus nattereri.* * The operculum of one specimen was not visible.

Osteological characters	Absent	Present
Ossification of tectum and solum nasi	12	4
Nasal overlapping sphenethmoid	3	13
Frontoparietals overlapping sphenethmoid	2	14
Posterior process of the vomer overlapping sphenethmoid	2	14
Posterior process of the vomer of different sizes	12	4
Cartilage in operculum	5	10
Left epicoracoid overlapping the right ventrally	4	12

The septum nasi is ossified in all males, but mineralization in the tectum and solum nasi varies. As judged by their relationship with the sphenethmoid, the lengths of the nasals, frontoparietals, and vomers vary. The relative size of the posterior processes of the vomer differs between the right and left sides of the same specimen. In one individual, the neopalatines did not overlie the anterior process of the pterygoid laterally, and the right neopalatine did not overlap the sphenethmoid medially. The occipital canal is totally roofed (i.e., closed) by the frontoparietal (like a tube), or partially to completely open (as a canal). The degree of enclosure of the occipital canal also varies contralaterally in the same specimen.

The hyali of two males have short, horn-like anterior processes. In three individuals, the base of the hyale has a cartilage expansion. The hyali of most specimens (N = 9) have both anterior processes and cartilage expansion. The region between the anterior ends of the posteromedial processes consistently is heavily mineralized. The distal ends of the bronchial processes have a variable number of subdivisions, ranging from two to four.

The left epicoracoid overlaps the right in most specimens. Epicoracoidal horns are visible in five individuals. One specimen has a simple (i.e., not bifurcate) mesosternum.

There is sexual dimorphism in some features. For example, the space between the posteromedial processes is not mineralized in the female, and the larynx is only about a quarter of that in males and has a simpler structure. The female also has additional cartilaginous prepollical elements.

Interspecific variation. A summary of the observed characters in *Physalaemus nattereri,* along with available osteological information for other species of *Physalaemus* are presented in Table 2.

TABLE 2. Comparison between *Physalaemus nattereri* and other species of *Physalaemus*. The literature information for *Physalaemus* species groups was summarized from Lobo (1992, 1996) and Nascimento *et al*. (2005). *Varies within the species group. gr. = Group.

Character	*P. nattereri*	Other *Physalaemus*
Ratio between the length and width of skull.	Wider than long.	Wider than long in *P.* gr. *cuvieri*, *P.* gr. *albifrons*, *P.* gr. *signifer*, *P.* gr. *ofersii* and *P.* gr. *henselii**. As wide as long in *P.* gr. *deimaticus* and longer than wide in *P.* gr. *gracilis*.
Contact between posterior border of nasals and sphenethmoid.	Present.	Present in all species groups except *P.* gr. *henseli*. In *P.* gr. *gracilis* and *P.* gr *olfersii* it varies.
Frontoparietal fontanelle.	Not exposed.	Exposed only in *P.* gr. *henselii**.
Posterior process of vomer.	Broad.	Broad in all species groups, except *P.* gr. *signifer*, *P.* gr. *henselii* and *P.* gr. *olfersii**. Reduced in *P.* gr. *deimaticus*.
Neopalatines.	Present.	Present in all species groups but *P.* gr. *deimaticus*. Reduced in *P.* gr. *henselii** and reduced or absent in *P.* gr. *signifer.*
Neopalatines overlapping the anterior process of the pterygoid.	Yes.	Not overlapping in all *Physalemus* species groups, except *P.* gr. *cuvieri* and *P.* gr. *albifrons*. And it varies in *P.* gr. *henselii.*
Anterior margin of prootic foramen.	Partially enclosed by prootics.	Completely enclosed by prootics in *P.* gr. *gracilis*, partially enclosed in *P.* gr. *cuvieri**, and not enclosed in *P.* gr. *albifrons* and *P.* gr. *signifer.* Variable in *P.* gr. *henselii*. There is no information for *P.* gr. *deimaticus* and *P.* gr. o*lfersii.*
Premaxillary and maxillary teeth.	Absent.	Present in all species groups except *P.* gr *deimaticus.* Varies in *P.* gr. *signifer*.
Position of the skull-mandible articulation.	Anterior to the intersection between the alae and cultriform process of parasphenoid.	Same level to the intersection between the alae and cultriform process of parasphenoid in *P.* gr. *cuvieri*, *P.* gr. *albifrons* and *P.* gr. *deimaticus*. Posterior in *P.* gr. *signifer*, *P.* gr. *gracilis*, *P.* gr *henselii* and *P.* gr. *olfersii.*
Angle between ventral ramus of squamosal and maxillary.	45º.	Less than 45º in *P.* gr. *gracilis*, equal or less than 45º in *P.* gr. *henselii*, approximately equal to 45º in *P.* gr. *olfersii*, and greater than 45º in *P.* gr. *cuvieri*, *P.* gr. *albifrons*, *P.* gr. *deimaticus*, and *P.* gr. *signifer.*
Anterior process of hyale.	Present.	Present in all species groups, except *P.* gr. *signifer**.
Constriction on the base of the anterolateral process of the hyoid.	Present.	Present in all species groups, except *P.* gr. *albifrons* and *P.* gr. *deimaticus.*
Mesosternum.	Bifurcated.	Bifurcated in all species groups, except *P.* gr. *henselii*. There is no information for *P.* gr. *deimaticus*, *P.* gr. *gracilis* and *P.* gr. *olfersii.*
Transverse process of the sacral diapophysis.	Posteriorly oriented.	Posteriorly oriented in *P.* gr. *cuvieri*, *P.* gr. *albifrons* and *P.* gr. *gracilis*. Transversely oriented in *P.* gr. *signifer* and *P.* gr. *henselii**. There is no information for *P.* gr. *deimaticus* and *P.* gr. *olfersii.*

Discussion

Variation and functionality of osteological traits. Osteological variation in *Physalaemus nattereri* mainly involves the amount of mineralization of cartilaginous elements (e.g., nasal capsule, hyoid, suprascapula) and the sizes of dermal elements (e.g., nasal, vomer). The increased mineralization observed in *Physalaemus nattereri* should not be confused with hyperossification found in other distantly related and large anurans such as *Pyxicephalus adspersus* Tschudi (Sheil 1999) or with miniaturization as exemplified by *Brachycephalus* Fitzinger (Campos *et al.* 2010). Instead, it resembles the condition characterizing other leptodactylid species that has been interpreted to be a reinforcement of the skull and related to digging habits in *Leptodactylus* Fitzinger (Heyer 1978; Ponssa 2008; Ponssa *et al*. 2010, 2011; Vera & Ponssa 2014).

The limited intraspecific variation described herein suggests that most osteological features are

phylogenetically and diagnostically reliable and therefore, useful in systematic studies as noted by previous investigations (e.g., Trueb 1977; Ponssa *et al*. 2011). Trueb (1977) suggested that the skull is an extremely conservative architectural unit owing to its role as the housing of the brain and sensory organs, as well as the mechanism for ingesting food—all of which are essential to the survival of the organism. The skull is usually considered more conserved than postcranial skeleton, but Trueb (1977) presented evidence of the low variation in the majority of the characters associated with the pectoral girdle and limbs. The variation of superficial dermal bones (e.g., sizes of the nasal bones and sphenethmoid, range of enclosed portion of the occipital canal) observed in this study was also noted by Trueb (1977) in a hylid species. So, the dimensions of superficial dermal roofing bones are considered least reliable as it depends on the size, sex, or age of specimens (Trueb 1977) and possibly homonal activity in early stages (Hanken & Hall, 1988; Hanken & Summers, 1988).

Leiuperines are included in the group of Type-IIA species (*sensu* Emerson 1979) or the lateral-bender morph (*sensu* Reilly & Jorgensen 2011) that have a laterally expanded sacral diapophysis and a broad dorsal iliosacral ligament (Emerson 1979, Reilly & Jorgensen 2011). As predicted, we found that *Physalaemus nattereri* has the same sacral diapophysis morphology as other leiuperines. This morphology is related to walking, burrowing, and/or hopping locomotion (Emerson 1979; Fabrezi *et al*. 2014). *Physalaemus nattereri* was reported to use the hind limbs for digging and typically is fossorial for at least part of the year (Toledo *et al*. 2011). Because the movements required for burrowing and for walking/jumping are similar, Emerson (1976) stated that burrowing hind-feet first into the substrate has required few adaptative changes; we found no striking features that could be beneficial to this locomotion mode. However, *P. nattereri* has a few osteological features that might facilitate the underground movement, although they are not exclusively related to this behaviour, such as the presence of an ossified septum nasi and well-developed humeral crests.

Among the morphological characters used by Nascimento *et al*. (2005) to define a monotypic genus in which to place *Physalaemus nattereri* was the anterior position of the skull-mandible articulation (Table 2). This character state was coded as either anterior to the intersection between the alae and cultriform process of parasphenoid for *Physalaemus nattereri*, or at the same level or posterior to the intersection between the alae and cultriform process of parasphenoid in other members of the genus (Nascimento *et al.* 2005). Therefore, this anatomical feature, which is associated with the amplitude of the mouth opening, is autapomorphic for *P. nattereri*, and may reflect a tendency to dietary specialization. Such an association has been made for larger species as ceratophryines that are characterized by a suite of morphological skull traits associated with feeding on large prey, among them, a jaw articulation posterior to the craniovertebral joint (Fabrezi & Emerson 2003; Fabrezi 2006; Fabrezi & Lobo 2009). Similar associations exist for smaller anurans that are burrowers and ones that specialize in small prey. Commonly, these species are edentate and have an anterior jaw articulation; they have relatively narrow mouths and actively search for prey (e.g., *Hemisus* Günther, *Rhinophrynus* Duméril & Bibron) (Schwenk 2000; Trueb & Cannatella, 1982; Trueb & Gans, 1983). Leptodactylids typically include a large diversity of prey in their diets (Parmlee 1999). In contrast, species of Leiuperinae—including *P. nattereri*—feed mostly on small prey items, such as termites and ants (Santos *et al*. 2003; Santana & Juncá 2007; Araújo *et al*. 2009; Rodrigues & Santos-Costa 2014; Oliveira *et al*. 2015).

Relationship between *Physalaemus nattereri* and its congeners. *Physalaemus nattereri* has been allied with the *P. biligonigerus* Group (Lynch 1970) and placed in a monotypic genus (Nascimento *et al*. 2005) based on morphological characters (external and osteological). It also has been included in phylogenetic studies, but mostly as an outgroup and along with few other *Physalaemus* species (Pyron & Wiens 2011; Faivovich *et al*. 2012; Fouquet *et al*. 2013; de Sá *et al*. 2014). A current, broad-sample phylogenetic hypothesis based on molecular evidence nests *P. nattereri* in the *P. signifer* Clade *sensu* Lourenço *et al.* (2015) that is defined by two putative morphological synapomorphies—viz., possession of a dark, arrowhead-shaped mark on the dorsum and the telocentric Chromosome 11 (Lourenço *et al.* 2015).

The *Physalaemus siginifer* Clade *sensu* Lourenço *et al.* (2015) includes *P. nattereri* as sister group of the *P. signifer* + *P. deimaticus* clades, former phenetic species groups *sensu* Nascimento *et al.* (2005). Given the osteological description presented here for *P. nattereri*, the information from literature (Table 1), and the aforementioned phylogenetic framework, there are a few anatomical characters shared by these species that could have further phylogenetic implications. Absence of premaxillary and maxillary teeth is an exclusive feature and possible synapomorphy of the *P. signifer* Clade sensu Lourenço *et al.* (2015), with secondary transformation within the *P. signifer* Group. Two characters are shared by the *P. deimaticus* and *P. signifer* groups, although not

exclusively—neopalatine reduction and an angle greater than 45º between ventral ramus of squamosal and maxilla. Last, the anterior position of the skull-mandible articulation is exclusive to *P. nattereri,* as proposed by Nascimento *et al.* (2005).

The skeletal morphology is heterogeneous within *Physalaemus* (Table 2); thus, it is difficult to infer species affinities. However, this overview of the osteology of *Physalaemus nattereri* is a starting point for the discussion of morphological transformation series and putative synapomorphies within *Physalaemus* and it underscores the need to include morphological, osteological, and molecular data to elucidate evolutionary changes within the genus. These results provide important characters for future studies on morphological variation, evolutionary relationships, and evolution of shape changes in *Physalaemus*.

Acknowledgments

We would like to thank B. Jennings, J.P. Pombal Jr., C. Canedo, M.C.S. Cardoso, S.P. Carvalho-e-Silva, and two anonymous reviewers for the suggestions that greatly improved this manuscript. J.P. Pombal Jr. (MNRJ) also facilitated our clearing-and-staining and examining specimens. We also thank T. Ferreira dos Santos for the line drawings in Figures 1A, 1B, and 1C. Martins Feitosa for providing access to the Leica M205 FA. Financial support was provided by CNPq and FAPERJ. ACCL thanks FAPESP for the fellowship received (grant 2012/25427-4). JF and MWC thanks CAPES for the scholarships received.

References

Aquino, L., Reichle, S., Silvano, D. & Scott, N. (2004) *Physalaemus nattereri*. The IUCN Red List of Threatened Species 2004: e.T57267A11597340. Available from: http://www.iucnredlist.org/details/biblio/57267/0 (accessed 20 November 2016)

Araújo, M.S., Bolnick, D.I., Martinelli, L.A., Giaretta, A.A. & dos Reis, S.F. (2009) Individual-level diet variation in four species of Brazilian frogs. *Journal of Animal Ecology*, 78, 848–856. https://doi.org/10.1111/j.1365-2656.2009.01546.x

Boulenger, G.A. (1888) XXIII.—Descriptions of new Brazilian batrachians. *Journal of Natural History*, 1, 187–189. https://doi.org/10.1080/00222938809460705

Campos, L.A., da Silva, H.R. & Sebben, A. (2010) Morphology and development of additional bony elements in the genus *Brachycephalus* (Anura: Brachycephalidae). *Biological Journal of the Linnean Society*, 99, 752–767. https://doi.org/10.1111/j.1095-8312.2010.01375.x

de Sá, R.O., Grant, T., Camargo, A., Heyer, W.R., Ponssa, M.L. & Stanley, E. (2014) Systematics of the neotropical genus *Leptodactylus* Fitzinger, 1826 (Anura: Leptodactylidae): phylogeny, the relevance of non-molecular evidence, and species accounts. *South American Journal of Herpetology*, 9, S1–S100. https://doi.org/10.2994/SAJH-D-13-00022.1

Emerson, S.B. (1976) Burrowing in frogs. *Journal of Morphology*, 149, 437–458. https://doi.org/10.1002/jmor.1051490402

Emerson, S.B. (1979) The ílio-sacral articulation in frogs: form and function. *Biological Journal of Linnean Society*, 11, 153–168. https://doi.org/10.1111/j.1095-8312.1979.tb00032.x

Emerson, S.B. (1982) Frog postcranial morphology: identification of a functional complex. *Copeia*, 3, 603–613. https://doi.org/10.2307/1444660

Fabrezi, M. (1992) El carpo de los anuros. *Alytes*, 10, 1–29.

Fabrezi, M. (1993) The anuran tarsus. *Alytes*, 11, 47–63.

Fabrezi, M. (1996) Las falanges terminales en la clasificación de los anuros. *Cuadernos de Herpetología*, 10, 1–9.

Fabrezi, M. (2006) Morphological evolution of Ceratophryinae (Anura, Neobatrachia). *Journal of Zoological Systematics and Evolutionary Research*, 44, 153–166. https://doi.org/10.1111/j.1439-0469.2005.00349.x

Fabrezi, M. & Emerson, S.B. (2003) Parallelism and convergence in anuran fangs. *Journal of Zoology*, 260, 41–51. https://doi.org/10.1017/S0952836903003479

Fabrezi, M. & Lobo, F. (2009) Hyoid skeleton, its related muscles, and morphological novelties in the frog *Lepidobatrachus* (Anura, Ceratophryidae). *The Anatomical Record*, 292, 1700–1712. https://doi.org/10.1002/ar.21014

Fabrezi, M., Manzano, A., Abdala, V. & Lobo, F. (2014) Anuran locomotion: ontogeny and morphological variation of a

distinctive set of muscles. *Evolutionary Biology*, 41, 308–326.
https://doi.org/10.1007/s11692-014-9270-y

Faivovich, J., Ferraro, D.P., Basso, N.G., Haddad, C.F.B., Rodrigues, M.T., Wheeler, W.C. & Lavilla, E.O. (2012) A phylogenetic analysis of *Pleurodema* (Anura: Leptodactylidae: Leiuperinae) based on mitochondrial and nuclear gene sequences, with coments on the evolution of anurans foam nests. *Cladistics*, 1 (2012), 1–23.
https://doi.org/10.1111/j.1096-0031.2012.00406.x

Fouquet, A., Blotto, B.L., Maronna, M.M., Verdade, V.K., Junca, F.A., de Sa, R. & Rodrigues, M.T. (2013) Unexpected phylogenetic positions of the genera *Rupirana* and *Crossodactylodes* reveal insights into the biogeography and reproductive evolution of leptodactylid frogs. *Molecular Phylogenetics and Evolution*, 67, 445–457.
https://doi.org/10.1016/j.ympev.2013.02.009

Halliday, T.R. & Verrell, P.A. (1988) Body size and age in amphibians and reptiles. *Journal of Herpetology*, 33, 253–265.
https://doi.org/10.2307/1564148

Hanken, J. & Hall, B.K. (1988) Skull development during anuran metamorphosis: I. Early development of the first three bones to form—the exoccipital, the parasphenoid, and the frontoparietal. *Journal of morphology*, 195, 247–256.
https://doi.org/10.1002/jmor.1051950303

Hanken, J. & Summers, C.H. (1988) Skull development during anuran metamorphosis: III. Role of thyroid hormone in chondrogenesis. *Journal of Experimental Zoology,* 246, 156–170.
https://doi.org/10.1002/jez.1402460208

Heyer, W.R. (1978) Systematics of the *fuscus* group of the frog genus *Leptodactylus* (Amphibia, Leptodactylidae). *Natural History Museum of Los Angeles County Science Bulletin*, 29, 1–85.

Lobo, F. (1992) Descripción osteológica de *Physalaemus fernanezae* (Anura: Leptodactylidae) y comparación con otras especies del género. *Acta Zoológica Lilloana*, 42, 51–53.

Lobo, F. (1995) Análisis filogenético del genero *Pseudopaludicola* (Anura: Leptodactylidae). *Cuadernos de Herpetología*, 9, 21–43.

Lobo, F. (1996) Nuevas observaciones sobre la osteología del género *Physalaemus* (Anura: Leptodactylidae). *Acta Zoológica Lilloana*, 43, 317–326.

Lourenço, L.B., Targueta, C.P., Baldo, D., Nascimento, J., Garcia, P.C., Andrade, G.V. & Recco-Pimentel, S.M. (2015) Phylogeny of frogs from the genus *Physalaemus* (Anura, Leptodactylidae) inferred from mitochondrial and nuclear gene sequences. *Molecular Phylogenetics and Evolution*, 92, 204–216.
https://doi.org/10.1016/j.ympev.2015.06.011

Lynch, J. (1970) Systematic status of the american Leptodactylid frog genera *Engystomops*, *Eupemphix* and *Physalaemus*. *Copeia*, 488–496.
https://doi.org/10.2307/1442276

Lynch, J. (1971) Evolutionary relationships, osteology and zoogeography of Leptodactyloid frogs. *University of Kansas Publications, Museum of Natural History, Miscellaneous Publications*, 53, 1–238.

Nascimento, L.B., Caramaschi, U. & Cruz, C.A.G. (2005) Taxonomic Review of the species groups of the genus *Physalaemus* Fitzinger, 1826 with revalidation of the genera *Engystomops* Jiménez-de-la-Espada, 1872 and *Eupemphix* Steindachner, 1863 (Amphibia, Anura, Leptodactylidae). *Arquivos do Museu Nacional*, 63, 297–320.

Oliveira, M., Gottschalk, M.S., Loebmann, D., Santos, M.B., Miranda, S., Rosa, C. & Tozetti, A.M. (2015) Diet composition and niche overlap in two sympatric species of *Physalaemus* (Anura, Leptodactylidae, Leiuperinae) in coastal subtemperate wetlands. *Herpetology Notes*, 8, 173–177.

Parmlee, J.R. (1999) Trophic Ecology of a Tropical Anuran Assemblage. *Scientific papers of Natural History Museum the University of Kansas*, 11, 1–59.

Ponssa, M.L. (2008) Cladistic analysis and osteological descriptions of the frog species in the *Leptodactylus fuscus* species group (Anura, Leptodactylidae). *Journal of Zoological Systematics and Evolutionary Research*, 46, 249–266.
https://doi.org/10.1111/j.1439-0469.2008.00460.x

Ponssa, M.L., Jowers, M. & de Sá, R. (2010) Osteology, natural history notes, and phylogenetic relationships of the poorly known Caribbean frog *Leptodactylus nesiotus* (Anura, Leptodactylidae). *Zootaxa*, 2646, 1–25.

Ponssa, M.L., Brusquetti, F. & Souza, F.L. (2011) Osteology and intraspecific variation of *Leptodactylus podicipinus* (Anura: Leptodactylidae), with comments on the relationship between osteology and reproductive modes. *Journal of Herpetology*, 45, 79–93.
https://doi.org/10.1670/09-190.1

Pugener, L.A. & Maglia, A.M. (2007) Skeletal morphology and development of the olfactory region of *Spea* (Anura: Scaphiopodidae). *Journal of Anatomy*, 211, 754–768.
https://doi.org/10.1111/j.1469-7580.2007.00826.x

Pyron, R.A. (2014) Biogeographic analysis reveals ancient continental vicariance and recent oceanic dispersal in amphibians. *Systematic Biology*, 63, 779–797.
https://doi.org/10.1093/sysbio/syu042

Pyron, R.A. & Wiens, J.J. (2011) A large-scale phylogeny of Amphibia including over 2800 species, and a revised classification of extant frogs, salamanders, and caecilians. *Molecular Phylogenetics and Evolution*, 61, 543–583.
https://doi.org/10.1016/j.ympev.2011.06.012

Reilly, S.M. & Jorgensen, M.E. (2011) The evolution of jumping in frogs: morphological evidence for the basal anuran locomotor condition and the radiation of locomotor systems in crown group anurans. *Journal of Morphology*, 272, 149–168.
https://doi.org/10.1002/jmor.10902

Rodrigues, L.C. & Santos-Costa, M.C. (2014) Trophic ecology of *Physalaemus ephippifer (*Anura, Leptodactylidae) in Eastern Amazonia. *Journal of Herpetology*, 48, 532–536.
https://doi.org/10.1670/13-142

Santana, A.S. & Juncá, F.A. (2007) Diet of *Physalaemus* cf. *cicada* (Leptodactylidae) and *Bufo granulosus* (Bufonidae) in a semideciduous forest. *Brazilian Journal of Biology*, 67, 125–131.
https://doi.org/10.1590/S1519-69842007000100017

Santos, J.W.A., Damasceno, R.P. & da Rocha, P.L.B. (2003) Feeding habits of the frog *Pleurodema diplolistris* (Anura, Leptodactylidae) in Quaternary sand dunes of the Middle Rio São Francisco, Bahia, Brazil. *Phyllomedusa*, 2, 83–92.
https://doi.org/10.11606/issn.2316-9079.v2i2p83-92

Sazima, I. & Caramaschi, U. (1986) Descrição de *Physalaemus deimaticus*, sp. n., e observações sobre comportamento deimático em *P. nattereri* (Steindn.)—Anura, Leptodactylidae. *Revista de Biologia*, 13, 91–101.

Schwenk, K. (2000) An introduction to Tetrapod feeding. *In*: Schwenk, K. (Ed.), *Feeding: Form, Function and Evolution in Tetrapod Vertebrates*. Academic Press, San Diego, pp. 102–116.
https://doi.org/10.1016/b978-012632590-4/50003-4

Sheil, C. (1999) Osteology and skeletal development of *Pyxicephalus adspersus* (Anura: Ranidae: Raninae). *Journal of Morphology*, 240, 49–75.
https://doi.org/10.1002/(SICI)1097-4687(199904)240:1%3C49::AID-JMOR5%3E3.0.CO;2-Z

Taylor, W.R. & Van Dyke, G.C. (1985) Revised procedures for staining and clearing small fishes and other vertebrates for bone and cartilage study. *Cybium*, 9, 107–119.

Toledo, L.F., Sazima, I. & Haddad, C.F.B. (2011) Behavioural defences of anurans: an overview. *Ethology Ecology and Evolution*, 23, 1–25.
https://doi.org/10.1080/03949370.2010.534321

Trueb, L. (1973) Bones, frogs, and evolution. *In*: Vial, J.L. (Ed.), *Evolutionary Biology of the Anurans: Contemporary Research on Major Problems*. University of Missouri Press, Columbia, pp. 65–132.

Trueb, L. (1977) Osteology of anuran sytematics: intrapopulational variation in *Hyla lanciformis. Systematic Zoology*, 26, 165–184.
https://doi.org/10.2307/2412839

Trueb, L. (1993) Patterns of cranial diversity among the Lissamphibia. *In*: Hanken, J. & Hall, B.K. (Eds.), *The Skull. Vol. 2. Patterns of structural and systematics diversity.* The University of Chicago Press, Chicago, pp. 255–343.

Trueb, L. & Cannatella, D.C. (1982) The cranial osteology and hyolaryngeal apparatus of *Rhinophrynus dorsalis* (Anura: Rhinophrynidae) with comparisons to recent pipid frogs. *Journal of Morphology*, 171, 11–40.
https://doi.org/10.1002/jmor.1051710103

Trueb, L. & Gans, C. (1983) Feeding specializations of the Mexican burrowing toad, *Rhinophrynus dorsalis* (Anura: Rhinophrynidae). *Journal of Zoology*, 199, 189–208.
https://doi.org/10.1111/j.1469-7998.1983.tb02090.x

Vera, M. & Ponssa, M.L. (2014) Skeletogenesis in anurans: cranial and postcranial development in metamorphic and postmetamorphic stages of *Leptodactylus bufonius* (Anura: Leptodactylidae). *Acta Zoologica (Stockholm)*, 95, 44–62.
https://doi.org/10.1111/azo.12007

APPENDIX I. Specimens examined.

Physalaemus nattereri: BRAZIL: Goiás (GO): MNRJ 24646, 24654, 24658, 24660, 24692, 25119–20; 25132–3, 40831; Mato Grosso do Sul (MS): MNRJ 13042; 13044; 13070, 31018; Minas Gerais (MG): MNRJ 22104, 57612; São Paulo (SP): MNRJ 69626.